INSTITUTE OF PHYSICS PUBLISHING JOURNAL OF PHYSICS B: ATOMIC, MOLECULAR AND OPTICAL PHYSICS

J. Phys. B: At. Mol. Opt. Phys. **38** (2005) 2775–2791 doi:10.1088/0953-4075/38/15/015

H_2^+ ionization by ultra-short electromagnetic pulses investigated through a non-perturbative Coulomb–Volkov approach

V D Rodríguez[1], P Macri[1,2] and R Gayet[3]

[1] Departamento de Física, FCEyN, Universidad de Buenos Aires, 1428 Buenos Aires, Argentina
[2] Instituto de Astronomía y Física del Espacio, Consejo Nacional de Investigaciones Científicas y Técnicas, 1428 Buenos Aires, Argentina
[3] CELIA (Centre Lasers Intenses et Applications (UMR 5107, Unité Mixte de Recherche CNRS-CEA-Université Bordeaux 1), Université Bordeaux 1, 351 Cours de la Libération, 33405 Talence Cedex, France

Received 20 May 2005, in final form 23 June 2005
Published 18 July 2005
Online at stacks.iop.org/JPhysB/38/2775

Abstract

The sudden Coulomb–Volkov theoretical approximation has been shown to well describe atomic ionization by intense and ultra-short electromagnetic pulses, such as pulses generated by very fast highly-charged ions. This approach is extended here to investigate single ionization of homonuclear diatomic molecules by such pulses in the framework of one-active electron. Under particular conditions, a Young-like interference formula can approximately be factored out. Present calculations show interference effects originating from the molecular two-centre structure. Fivefold differential angular distributions of the ejected electron are studied as a function of the molecular orientation and internuclear distance. Both non-perturbative and perturbative regimes are examined. In the non-perturbative case, an interference pattern is visible but a main lobe, opposite to the electric field polarization direction, dominates the angular distribution. In contrast, in perturbation conditions the structure of interferences shows analogies to the Young-like interference pattern obtained in ionization of molecules by fast electron impacts. Finally, the strong dependence of these Young-like angular distributions on the internuclear distance is addressed.

1. Introduction

In the immense field of processes induced by laser beams in matter, the ionization of molecules by ultra-short and intense laser pulses offers a vast menu of new phenomena such as interferences (Lein *et al* 2002a, Spanner *et al* 2004), molecular orientation dependence of angular distribution including alignment (Litvinyuk *et al* 2003, Lein *et al* 2002b, Ellert and

 © 2005 IOP Publishing Ltd Printed in the UK

Corkum 1999, Seideman 2002, Reid 2003), and inhibition of the ionization of a molecule in conditions where an atom with the same ionization potential would be ionized (Muth-Böhm *et al* 2000, Wells *et al* 2002). In laser physics, short pulses means subfemtosecond pulses. However, relativistic highly-charged ions can generate both the shortest and the most intense pulses ever achieved (Moshammer *et al* 1997). Then, one speaks of attosecond pulse times. In the present paper, we are interested in ionization of homonuclear molecules by such attosecond pulses. Indeed, one expects interference effects to show up.

Interference phenomena should occur when electrons are released from molecules interacting with a short electromagnetic pulse. Just like in a Young experiment, we can regard the atoms as photon absorbers, which play the role of separate and coherent sources of photoelectrons, thus leading to electronic interference patterns. For diatomic molecules, these patterns should show a periodicity that depends on the ratio of the internuclear distance to the photoelectron wavelength. Such electronic interferences can modulate the ionization cross sections. In the case of photoionization, interference phenomena have been identified for many years (Cohen and Fano 1966, Walter and Briggs 1999, Weber *et al* 2004). However, the observation of oscillations due to interferences in electron spectra produced by high-energy collisions of heavy ions with H_2 molecules was only made very recently (Stolterfoht *et al* 2001). In such experiments, it is difficult to see the oscillations because the cross sections fall off rapidly when the electron energy increases. In order to enhance visibility, the measured cross section was divided by twice the theoretical atomic ionization cross section of H atoms. Since the ratio strongly depends on relevant parameters of the theoretical model (e.g., effective charges), the appearance of the oscillations is difficult to interpret. More recently, ionization of both atomic and molecular hydrogen by heavy ion impacts at lower energies has been measured (Misra *et al* 2004) giving stronger evidence to the existence of interference patterns.

Experiments are generally performed on gas targets with a random molecular orientation, thus imposing severe restrictions on the comparison between theory and experiments. Recently, it has become possible to observe alignment-dependent ionization of N_2 (Litvinyuk *et al* 2003). Studying how the ionization rate, the photoelectron energy and the angular spectra depend on the orientation of the molecule should provide interesting piece of information for high harmonics yields (Lein *et al* 2002a) and for molecular dissociation (Ellert and Corkum 1999). Such studies should be useful in applications such control of ionization and dissociation pathways, rotational cooling, molecular trapping and pendular state spectroscopy (Seideman 2002, Reid 2003).

Theoretical (Muth-Böhm *et al* 2000) and experimental (Wells *et al* 2002) evidences on molecular ionization suppression have been recently reported. In the work of Muth-Böhm *et al* (2000), the suppression mechanism is related to the symmetry of molecular ground state.

Most processes that occur in the ionization of one-active electron atoms by short laser pulses may be well predicted by numerical methods that compute the solution of the full time-dependent Schrödinger equation (Cormier and Lambropoulos 1997, Muller and Kooiman 1998, Kondorskiy and Presnyakov 2001). However, it is no longer the case neither with high intensities and/or long pulse durations, nor with more complex systems such as molecules and many-electron atoms. At the same time, there is a need for robust analytical approaches both to interpret experimental data and to identify dominant mechanisms. In this context, the strong field approximation might appear as the basic reference (Keldysh 1965, Faisal 1973, Reiss 1980). Unfortunately, this approach and others introduced later (Well *et al* 2002, Muth-Böhm *et al* 2001) neglect the Coulomb interaction between the ejected electron and the residual ion, thus leading to an incorrect asymptotic behaviour of the final state which is a fundamental shortcoming as already demonstrated a long time ago (Dollard 1964). Further,

for the ionization of H atoms by ultra-short pulses, Duchateau *et al* (2000b) compared electron energy distributions obtained with Volkov plane waves (VS) to predictions of both, an accurate quantum numerical approach, and a classical trajectory Monte Carlo (CTMC) approach. These two later calculations give the same results but they do not agree with VS predictions, more specially close to the ionization threshold. As a way to get rid of this drawback, an analytical approach called CV1 appeared recently (Duchateau *et al* 2000a). It is based on the well-known Coulomb–Volkov (CV) wavefunctions (Jain and Tzoar 1978). When the interaction of an atomic system with an external field may be approximated by a dipolar term in the time-dependent Schrödinger equation, CV states show interesting properties: they are exact solutions of this equation either when the external field is zero or, for hydrogen-like atomic systems, when the nuclear charge is zero. Therefore, unlike Volkov states, CV wavefunctions show the required Coulomb asymptotic behaviour when the external field disappears. The first few applications of CV1 were made by Duchateau *et al* (2001, 2002) in the framework of the sudden approximation. CV1 gives predictions which agree well with quantum and CTMC calculations for the abovementioned ionization of H by ultra-short pulses (Duchateau *et al* 2000b). In fact, compared to exact computations, CV1 predictions were shown to be accurate and reliable as long as both, the pulse duration does not exceed half the initial state orbital period, and the electromagnetic field does not perform more than two optical cycles (Duchateau and Gayet 2001). At present, laser facilities can produce femto and sub-femto second pulses (Nisoli *et al* 1997, Duchateau *et al* 2003). Actually, the pulse duration given by experimentalists corresponds to the full width at half maximum (FWHM), i.e., the period of time where the laser field reaches its highest intensities. For the shortest pulses, CV1 can provide reliable predictions about ionization processes during this time for large enough principal quantum numbers n. For example, one should have $n > 4$ for the pulses produced a few years ago in Vienna (Nisoli *et al* 1997). The use of CV wavefunctions was later extended with success to longer and complete laser pulses with many field oscillations. It was done in a framework similar to a distorted wave approach (Duchateau *et al* 2003, Macri *et al* 2003). This later theoretical method was called CV2. An extension of CV2 called MCV2 (Modified CV2) has been able to explain conspicuous structures in the multiphoton ionization spectra (Rodríguez *et al* 2004). The origin of these structures was found in the contribution of intermediate bound states that can be excited by the laser (Rodríguez *et al* 2004). However, the application of CV1 to the ionization of hydrogen targets in the ground state requires pulse durations shorter than 8 attoseconds. Although such pulses are commonly generated by relativistic ions, they are still far from being produced with lasers.

In the present paper, the simplest approach CV1 is adapted to explore its ability of investigating the rich range of effects appearing in the ionization of molecules by ultra-short ion impacts. Since characteristic periods in molecular states are significantly longer than in atoms, one expects that it will accurately describe the many processes in a range of external field parameters more extended than in the case of atoms. Indeed, the model is kept in a very amenable form.

The paper is organized as follows: in section 2, we outline the model that is used here to study the interaction between a single-active electron molecule and a very short electromagnetic pulse. Results are presented in section 3. Conclusions and outlook are given in section 4. Atomic units are used throughout unless otherwise stated.

2. Theory

The interaction between a hydrogen-like target of nuclear charge Z_T and a bare projectile of nuclear charge Z_P is

$$V(\vec{r}, \vec{R}) = \frac{Z_P Z_T}{R} - \frac{Z_P}{\|\vec{R} - \vec{r}\|} = Z_P \left(\frac{1}{R} - \frac{1}{\|\vec{R} - \vec{r}\|} \right) + \frac{Z_P (Z_T - 1)}{R} \tag{1}$$

where $\vec{r}$ and $\vec{R}$ are the positions of the electron and of the projectile with respect to the target nucleus respectively. To match the required asymptotic forms in the case of collisions without rearrangement (excitation or ionization), the long-range ion–ion interaction $Z_P(Z_T - 1)/R$ has to be taken into account in the entrance and exit channel-states. Then, the interaction $\bar{V}(\vec{r}, \vec{R})$ that can induce a transition is the first term of the right-hand side of (1). For high projectile charges and very high impact velocities, it is well known that excitation and ionization processes are dominated by distant collisions, i.e., for $R \gg r$. In this case, $\bar{V}(\vec{r}, \vec{R})$ is well represented by the dipolar term (Rodriguez and Falcon 1990). This dipolar term is

$$\bar{V}_D(\vec{r}, \vec{R}) = -Z_P \frac{\vec{r} \cdot \vec{R}}{R^3} = -\vec{d} \cdot F(\vec{R}) \tag{2}$$

where $\vec{d} = -\vec{r}$ is the atomic dipole and $\vec{F}(\vec{R})$ is the electric field generated by the projectile at the target nucleus. According to (2), one has

$$\vec{F}(\vec{R}) = -Z_P \frac{\vec{R}}{R^3}. \tag{3}$$

When the impact velocity $\vec{v}$ is high, the projectile trajectory is in almost straight line. Thus $\vec{R}$ may be written as

$$\vec{R} = \vec{\rho} + \vec{v}\, t \tag{4}$$

where $\vec{\rho}$ is the impact parameter and t is the time whose origin is at the closest distance of approach. Therefore, $\vec{F}(\vec{R})$ is now

$$\vec{F}(\vec{\rho},\ t) = -Z_P \frac{\vec{\rho} + \vec{v}\, t}{(\rho^2 + v^2 t^2)^{3/2}}. \tag{5}$$

From expression (5) $\vec{F}(\vec{\rho},\ t)$ appears as a time-derivative of a vector potential $\vec{A}(\vec{\rho},\ t)$:

$$\vec{F}(\vec{\rho},\ t) = -\frac{\partial \vec{A}(\vec{\rho},\ t)}{\partial t} \tag{6}$$

with

$$\vec{A}(\vec{\rho},\ t) = \frac{Z_P}{v} (\rho^2 + v^2\, t^2)^{-1/2} \left(\hat{\rho} \frac{v\, t}{\rho} - \hat{v} \right) + \vec{A}_0. \tag{7}$$

In (7), $\hat{v}$ and $\hat{\rho}$ are the unit vectors along and perpendicular to the trajectory respectively while $\vec{A}_0$ is a time-independent vector. Therefore, transitions that may be induced by the field $\vec{F}(\vec{R})$ fall within the frame of interactions with electromagnetic fields. Since we are interested in ionization by very fast ions, we may address this process through the CV1 approach introduced by Duchateau *et al* (2000a, 2000b) in the framework of the sudden approximation. To calculate the CV1 transition amplitude, one needs to know the whole variation of the vector potential during the interaction, no matter what the vector potential is during this time. According to (7), the variation of $\vec{A}(\vec{\rho},\ t)$, during a collision, is

$$\Delta \vec{A} = \frac{2 Z_P}{\rho v} \hat{\rho}. \tag{8}$$

Only the transverse component of $\vec{A}$ contributes to $\Delta \vec{A}$. Such a situation is comparable to the effect of a half-cycle pulse of a linearly polarized laser. With reference to the collision system studied by Moshammer *et al* (1997), we represent in figure 1 the transverse component of the field created at the nucleus of a target atom by a 1 GeV/nucleon U^{92+} ion. The corresponding

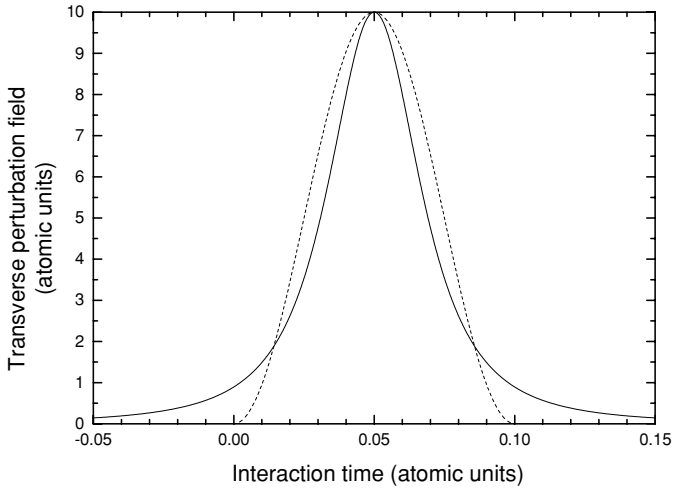

Figure 1. The full line represents the transverse electric field generated by a 1 GeV/nucleon U^{92+} at the nucleus of an atomic target as a function of time. The closest distance of approach $\rho \approx 3$ au is reached at $t = 0.05$ au. The dashed line simulates the previous ion field by means of a sine-square function that is zero outside the range $[0, 0.1]$. The two pulses have similar vector potential variations (see text).

velocity is $v = 120$ au. The maximum value of the field, that is reached at $t = 0.05$ au ($\approx$1 as), corresponds to an impact parameter $\rho \simeq 3$ au. Such a field is equivalent to an electromagnetic flux 3.5×10^{18} W cm^{-2}. In the present example, more than 90% of the variation of the transverse vector potential is obtained between 0 and $\tau = 0.1$ au, i.e., in a time $\tau \approx 2.5$ as. As shown in figure 1, one may simulate this pulse by a sine-square function restricted to the range $[0, \tau]$, whose integral is very close to the value given by (8). Such sine-square functions always enable us to nicely reproduce the variation of the transverse vector potential of very fast ions. Therefore, they have been employed in the present study of ion impact induced ionization of homonuclear molecules. In fact, our analysis remains valid for any projectile charge provided that the impact parameter and the impact velocity are scaled according to the rules established by Rodriguez and Falcon (1990).

We consider here the ionization of a one-active electron homonuclear molecule by an external electric field $\vec{F}(\vec{r}, t)$ supposed to be homogenous in the volume of the molecule, thus permitting us to write $\vec{F}(\vec{r}, t) = F(t)$ in this volume. Under non-relativistic conditions and within the electric dipole approximation, the wavefunction $\Psi(\vec{r}, t)$ of the outermost electron satisfies the time-dependent Schrödinger equation:

$$\begin{aligned} \mathrm{i}\,\frac{\partial \Psi(\vec{r},\, t)}{\partial t} &= [H_m + \vec{r}\cdot\vec{F}(t)]\Psi(\vec{r},\, t) \\ H_m &= -\frac{\nabla^2}{2} + V_m(\vec{r}, \vec{\rho}) \end{aligned} \tag{9}$$

where $\vec{\rho}$ is the internuclear distance and $\vec{r}$ is the position of the electron with respect to the mid-point between nuclei; this mid-point is identified with the centre of mass. In the frozen core approximation $V_m(\vec{r}, \vec{\rho})$ is a model potential that simulates the potential experimented by the outermost active electron (Duchateau *et al* 2001, Galassi *et al* 2002). The model potential may generally be taken as

$$V_m(\vec{r}, \vec{\rho}) = \frac{Z_T}{r_a} + \frac{Z_T}{r_b} + V_p(\vec{r}, \vec{\rho}) \tag{10}$$

where $\vec{r}_{a,b} = \vec{r} \pm \vec{\rho}/2$ are the positions of the electron with respect to nuclei a and b, respectively. Thus, $V_p(\vec{r}, \vec{\rho})$ represents the average influence of the passive electrons of the core on the active electron. In an ionizing process, the initial bound state $\phi_i(\vec{r}, \vec{\rho}, t)$ and the final continuum state $\phi_f^-(\vec{r}, \vec{\rho}, t)$ may be written as

$$\begin{aligned} \phi_i(\vec{r}, \vec{\rho}, t) &= \varphi_i(\vec{r}, \vec{\rho}) \exp(-\mathrm{i}\varepsilon_i t) \\ \phi_f^-(\vec{r}, \vec{\rho}, t) &= \varphi_f^-(\vec{r}, \vec{\rho}) \exp(-\mathrm{i}\varepsilon_f t). \end{aligned} \tag{11}$$

In the present work we focus on the molecular ion H_2^+ although the formalism remains valid for any one-active electron system where a reasonable model or pseudo-potential $V_m(\vec{r}, \vec{\rho})$ may be used to represent the interaction of the active electron with the rest of the system. The initial active-electron wavefunction $\varphi_i(\vec{r})$ is approximated here by a linear combination of atomic orbitals (LCAO) with two variational single-zeta functions,

$$\begin{aligned} &\varphi_i(\vec{r}, \vec{\rho}) \cong N(\rho)\,[\varphi_A(r_a)\,\varphi_B(r_b) + \varphi_B(r_a)\,\varphi_A(r_b)] \qquad \text{where} \\ &\varphi_M(r_n) = \exp(-Z_M r_n) \qquad \text{with} \quad M = A, B \quad \text{and} \quad n = a, b \end{aligned} \tag{12}$$

where $Z_{A,B}$ are the variational parameters and $N(\rho)$ is the normalization factor. In the present case we have $Z_A = 0.224\,086$, $Z_B = 1.136\,03$ at the equilibrium internuclear distance $\rho = 2$ au and $N(\rho) = 0.614\,2109$. Following Joulakian *et al* (1996), we assume that the ejected electron may be described by a two-centre continuum wavefunction given by

$$\begin{aligned} \varphi_f^-(\vec{r}) &= \frac{\mathrm{e}^{\mathrm{i}\vec{k}\cdot r}}{(2\pi)^{3/2}} \psi_{\vec{k}}^-(\vec{r}_a, t)\, \psi_{\vec{k}}^-(\vec{r}_b, t) \\ \psi_{\vec{k}}^-(\vec{r}_j, t) &= \exp(\pi\nu/2)\Gamma(1 + \mathrm{i}\nu)\, {}_1F_1(-\mathrm{i}\nu, 1, -\mathrm{i}kr_j - \mathrm{i}\vec{k}\cdot\vec{r}_j) \end{aligned} \tag{13}$$

where $\nu = 1/k$, and ${}_1F_1$ is the confluent hypergeometric function. This wavefunction satisfies exact limit of the outgoing wave in the field of the two nuclei (Joulakian *et al* 1996). Calculations performed with the approximate wavefunctions (12) and (13) by Joulakian *et al* (1996) for the ionization of H_2^+ by electron impacts have been compared with predictions made by Serov *et al* (2002) using exact numerical bound and continuum wavefunctions. Both calculations agree reasonably well, in particular for forward electron scattering.

A sine-square envelope shapes the finite pulse. Thus, in the vicinity of the molecular ion the external electric field reads

$$\begin{cases} \vec{F}(t) = \vec{F}_0 \sin^2\left(\dfrac{\pi t}{\tau}\right) & \text{when} \quad t \in [0, \tau] \\ \vec{F}(t) = \vec{0} & \text{elsewhere} \end{cases} \tag{14}$$

where τ is the total duration of the pulse. In the Coulomb gauge, the electric field of a propagating electromagnetic wave is the opposite time-derivative of a vector potential $\vec{A}(t)$ that may be written as

$$\vec{A}(t) = \vec{A}(t_0) - \int_{t_0}^{t} \mathrm{d}t'\, \vec{F}(t'). \tag{15}$$

In the Schrödinger picture, the transition amplitude from the state i at $t = 0$ to the final state f at $t = \tau$ is given by the general expression:

$$a_{fi}^- = \left\langle \chi_f^-(\vec{r}, t) \middle| \chi_i^+(\vec{r}, t) \right\rangle \tag{16}$$

where $\chi_f^-(\vec{r}, t)$ and $\chi_i^+(\vec{r}, t)$ are the exact incoming and outgoing solutions of equation (9) respectively. These solutions are subject to the following asymptotic conditions:

$$\chi_f^-(\vec{r}, t) \underset{t \geqslant \tau}{\longrightarrow} \phi_f^-(\vec{r}, \vec{\rho}, t) \tag{17a}$$

$$\chi_i^+(\vec{r},t) \underset{t\leqslant 0}{\longrightarrow} \phi_i(\vec{r},\vec{\rho},t). \tag{17b}$$

Expression (16) provides two usual forms of the exact transition amplitude: (i) at $t = 0$ when $\chi_f^-(\vec{r},t)$ is an exact solution of (9) while $\chi_i^+(\vec{r},t) = \phi_i(\vec{r},t)$ and (ii) at $t = \tau$ when $\chi_i^+(\vec{r},t)$ is an exact solution of (9) while $\chi_f^-(\vec{r},t) = \phi_f^-(\vec{r},t)$. In the so-called CV1 approximation, a Coulomb–Volkov wavefunction (Duchateau *et al* 2000a, 2000b, 2001) is used in place of the required exact solution either at $t = 0$ or at $t = \tau$. Both approaches are shown to provide identical predictions. It is worth pointing out that CV1 results for hydrogen ionization by ultra-short electromagnetic pulses have been found reliable whenever the sudden approximation holds, i.e., when the pulse duration is smaller than a lapse of time characteristic of the initial electronic state evolution (Duchateau *et al* 2000a, 2000b). In what follows, we use the amplitude at $t = 0$ that is called CV1$^-$. In CV1$^-$, the wavefunction $\chi_f^-(\vec{r},t)$ is approximated by the following Coulomb–Volkov wavefunction:

$$\begin{cases} \chi_f^-(\vec{r},t) = \phi_f^-(\vec{r},\vec{\rho},t)L^-(\vec{r},t) \\ L^-(\vec{r},t) = \exp\left\{ \mathrm{i}\vec{A}^-(t)\cdot\vec{r} - \mathrm{i}\vec{k}\cdot\displaystyle\int_\tau^t \mathrm{d}t'\,\vec{A}^-(t') - \frac{\mathrm{i}}{2}\int_\tau^t \mathrm{d}t'\,\vec{A}^{-2}(t') \right\} \end{cases} \tag{18}$$

where $\vec{A}^-(t)$ is the variation of $\vec{A}(t)$ over the time interval $[\tau, t]$, i.e.,

$$\vec{A}^-(t) = -\int_\tau^t \vec{F}(t)\,\mathrm{d}t \tag{19}$$

and where $\chi_i^+(\vec{r}, t = 0) = \phi_i^+(\vec{r}, t = 0)$. Introducing the wavefunction (12) in the expression (16), the transition amplitude CV1$^-$ may be written, after an easy algebra, as

$$a_{fi}^{\mathrm{CV1-}} = N(\rho)\exp(\mathrm{i}\phi)\int \mathrm{d}\vec{r}\exp[-\mathrm{i}\,\vec{q}\cdot\vec{r}]\varphi_f^{-*}(\vec{r},\vec{\rho})\,[\varphi_A(r_a)\varphi_B(r_b) + \varphi_B(r_a)\varphi_A(r_b)] \tag{20}$$

where $\vec{q}$ is the momentum transferred by the electric field to the electron and ϕ is the following constant phase that leaves the probability unchanged:

$$\phi = \vec{k}\cdot\int_\tau^0 \mathrm{d}t'\,\vec{A}^-(t') + \frac{1}{2}\int_\tau^0 \mathrm{d}t'\,\vec{A}^{-2}(t') \qquad \vec{q} = \vec{A}^-(0). \tag{21}$$

We first examine the integrals over coordinates in (20). Following the procedure of Joulakian *et al* (1996), the integral is transposed to the momentum space. After a lengthy, but otherwise straightforward procedure, the result is

$$a_{fi}^{\mathrm{CV1-}} = N(\rho)\exp(\mathrm{i}\phi)\,(\exp(-\mathrm{i}\,(\vec{q}-\vec{k})\cdot(\vec{\rho}/2))A(\vec{q},\vec{\rho}) + \exp(\mathrm{i}(\vec{q}-\vec{k})\cdot(\vec{\rho}/2))A(\vec{q},-\vec{\rho})) \tag{22}$$

where one has

$$A(\vec{q},\vec{\rho}) = \int \mathrm{d}\vec{Q}\,\mathrm{e}^{-\mathrm{i}\vec{Q}\cdot\vec{\rho}}W(\vec{k},\vec{Q},Z_A)\,W(\vec{k},\vec{k}-\vec{q}-\vec{Q},Z_B). \tag{23}$$

In (23), $W(\vec{k},\vec{V},Z_M)$ with $M = A, B$ and $\vec{V} = \vec{Q}, \vec{k}-\vec{q}-\vec{Q}$ is a form factor-like function:

$$W(\vec{k},\vec{K},Z_M) = \int \mathrm{d}\vec{r}\,\mathrm{e}^{-\mathrm{i}\vec{k}\cdot\vec{r}}\,\mathrm{e}^{-Z_M r}\,{}_1F_1(-\mathrm{i}\nu,1,\mathrm{i}kr+\mathrm{i}\vec{k}\cdot\vec{r}) \tag{24a}$$

$$W(\vec{k},\vec{V},Z_M) = \frac{4\pi}{V^2+Z_M^2}\left(1+\frac{2\vec{k}\cdot\vec{V}-2\mathrm{i}Z_Mk}{V^2+Z_M^2}\right)^{\mathrm{i}\nu}\left\{2(1+\mathrm{i}\nu)-\frac{2\nu(k+\mathrm{i}Z_M)}{(\vec{V}+\vec{k})^2-(k+\mathrm{i}Z_M)^2}\right\}. \tag{24b}$$

Expression (24*b*) is easily obtained through a standard Nordsieck-type integration (Nordsieck 1954). Note that expression (24*a*) features an electronic transition from a bound state 1s with a binding charge Z_M, to the continuum. However, the amplitude $A(\vec{q},\vec{\rho})$ is a convolution of two form factors. This rather general result leads to the CV1 transition amplitude (22) that is a sum of two ionization amplitudes weighted by a specific phase factor. It reflects the fact that the electron can be emitted from any centre. Now, the main contributions to the integral over $\vec{Q}$ in (23), come from the neighbourhoods of $\vec{Q}=\vec{0}$ and $\vec{Q}=\vec{k}-\vec{q}$. For large values of the electric field F_0, the norm of the momentum transfer $\vec{q}=\vec{A}^-(t=0)$ may be large (e.g., with half-cycle pulses). In this case, the integrant in (23) exhibits two peaks a long way apart, thus permitting us to approximate expression (23) as

$$A(\vec{q},\vec{\rho}) \approx W(\vec{k},\vec{k}-\vec{q},Z_B)\int \mathrm{d}\vec{Q}\,\mathrm{e}^{-\mathrm{i}\vec{Q}\cdot\vec{\rho}}W(\vec{k},\vec{Q},Z_A) + W(\vec{k},\vec{k}-\vec{q},Z_A)\int \mathrm{d}\vec{Q}\,\mathrm{e}^{-\mathrm{i}\vec{Q}\cdot\vec{\rho}}\,W(\vec{k},\vec{k}-\vec{q}-\vec{Q},Z_B). \tag{25}$$

Using (24*b*), it is easy to show that, for the values of $q=\|\vec{q}\|$ larger than any other quantity, each factor outside the integrals in (25) may be approximated as

$$W(\vec{k},\vec{q}-\vec{k},Z_M) \approx \frac{8\pi(1+\mathrm{i}\nu)}{(\vec{q}-\vec{k})^2+Z_M^2} \qquad \text{with} \quad M=A,B. \tag{26}$$

Since q is large, Z_M^2 may be ignored in (26), thus leading to a common factor, whose effect is to reduce the contributions of the two peaks in the CV1 amplitude.

Further, it is clear that the maximum value of $A(\vec{q},\vec{\rho})$ is reached when $\vec{k}=\vec{q}$ because both functions W in the integrant are maximum for $\vec{Q}=\vec{0}$. Therefore, one expects a peak in the electron energy spectrum at an energy corresponding to $\vec{k}=\vec{q}$. This result is consistent with a previous work (Duchateau *et al* 2000a, 2000b) where it is shown that the maximum in electron energy spectra is close to $E=\frac{\vec{A}^-(0)^2}{2}=\frac{\vec{q}^2}{2}$.

Now, starting from expressions (22) and (23) and making the following assumption

$$A(\vec{q},\vec{\rho}) \approx A(\vec{q},-\vec{\rho}) \approx A(\vec{q},0) \tag{27}$$

we can get the so-called two-effective centre (TEC) approximation (Weck *et al* 2001). The approximation (27) may be justified as follows: the analytical form (24*b*) shows that, given the small value of Z_A compared to Z_B, $W(\vec{k},\vec{Q},Z_A)$ is much more peaked at $\vec{Q}=\vec{0}$ than $W(\vec{k},\vec{k}-\vec{q}-\vec{Q},Z_B)$ at $\vec{Q}=\vec{q}-\vec{k}$. Therefore, in expression (23), one may replace $\mathrm{e}^{-\mathrm{i}\vec{Q}\cdot\vec{\rho}}$ by its value close to $\vec{Q}=\vec{0}$, i.e., by 1. Such a procedure is equivalent to taking $\vec{\rho}=\vec{0}$ in (23). Thus, the two-effective centre approximation (TEC) may be traced back to a peaking approximation in the integral (23). Introducing this approximation in (22) leads, after simple calculations, to the following TEC transition amplitude:

$$a_{fi,\mathrm{TEC}}^{\mathrm{CV1-}} \approx 2N(\rho)\exp(\mathrm{i}\phi)\cos[(\vec{q}-\vec{k})\cdot(\vec{\rho}/2)]A(\vec{q},0) \tag{28}$$

where

$$A(\vec{q},0) = C\int \mathrm{d}\vec{r}\,\mathrm{e}^{-\mathrm{i}(\vec{k}-\vec{q})\cdot\vec{r}}\,\mathrm{e}^{-(Z_A+Z_B)r}\,{}_1F_1(\mathrm{i}\nu,1,\mathrm{i}kr+\mathrm{i}\vec{k}\cdot\vec{r})\,{}_1F_1(\mathrm{i}\nu,1,\mathrm{i}kr+\mathrm{i}\vec{k}\cdot\vec{r}) \tag{29}$$

$$C=(2\pi)^3\exp(\pi\nu)\Gamma(1-\mathrm{i}\nu)^2. \tag{30}$$

An analytical expressions for (29) is also obtained through the above-mentioned procedure (Nordsieck 1954). It is worth noting that using a single Z function for the initial bound state and a single continuum wavefunction for the final state corresponds to the CV1 transition amplitude for ionization of any single centre of the molecule as if the atom were alone. Thus,

expression (28) exhibits Young-type interferences between the ionization amplitudes of the two centres. We would like to point out that analogous expressions have been found previously within the strong field approximation (SFA) (Muth-Böhm *et al* 2000, 2001) and more recently in the context of molecular ionization by impacts of, either heavy ions (Stolterfoht *et al* 2001) or electrons (Stia *et al* 2003). However, the present calculations differ from SFA ones because SFA uses a Volkov plane wave for the final wavefunction. It is noteworthy that expressions similar to (23) are derived by Stolterfoht *et al* (2001) and Weck *et al* (2001), both works making use of the so-called two-effective centre approximation. The integration over the electron coordinates may be expressed in terms of the well-known bound-continuum form factor. This form factor is analytical for hydrogen atoms (Joulakian *et al* 1996). Then, the fivefold differential ionization probability (FDIP) is given by

$$\frac{\partial^5 P_{fi}^{\mathrm{CV1-}}}{\partial E_K \partial \Omega_k \partial \Omega_\rho} = k \left| a_{fi}^{\mathrm{CV1-}} \right|^2 \tag{31}$$

where E_k and Ω_k are the energy and the direction of the impulse $\vec{k}$ of the ejected electron respectively; while Ω_ρ defines the orientation of the molecular axis vector $\vec{\rho}$.

Within the two-effective centre approximation the FDIP reads

$$\frac{\partial^5 P_{fi,\mathrm{TEC}}^{\mathrm{CV1-}}}{\partial E_K \partial \Omega_k \partial \Omega_\rho} = 4kN(\rho)^2 \cos^2\left[(\vec{k}-\vec{q})\cdot\frac{\vec{\rho}}{2}\right] |A(\vec{q},0)|^2. \tag{32}$$

Always within TEC, we may average over the molecular orientation thus obtaining

$$\frac{\partial^3 P_{fi,\mathrm{TEC}}^{\mathrm{CV1-}}}{\partial E_K \partial \Omega_k} = \frac{k}{2\pi} N(\rho)^2 |A(\vec{q},0)|^2 \left(1 + \frac{\sin[|\vec{k}-\vec{q}|\rho]}{|\vec{k}-\vec{q}|\rho}\right). \tag{33}$$

Integrating over Ω_k provides the energy distribution $\frac{\partial P_{fi}}{\partial E_K}$. A further integration over E_k yields the total ionization probability P_{ion}.

3. Results and discussion

In this work, H_2^+ differential ionization probabilities are computed for electrons emitted in a plane defined by the molecular axis and the z-axis taken in the direction of the linear polarization of the external field. Therefore, in all figures, 0° is the direction of the field. Calculations with the molecular CV1 theory introduced in section 2 are performed for a duration of the electromagnetic pulse $\tau = 5$ au. With atoms, such values of these parameters guarantee a good agreement between CV1 and exact numerical solutions of the time-dependent Schrödinger equation (Duchateau *et al* 2000a, 2000b, 2001). Since the ionization potential of neutral molecules is smaller than that of atoms, one expects the sudden condition to be better satisfied in the case of molecules.

The non-perturbative regime is first addressed with a pulse amplitude $F_0 = 1$ au. Calculations are then performed within the perturbation regime for different electron energies and various internuclear axis orientations. Finally, the issue of the dependence on the internuclear distance is analysed.

3.1. Non-perturbative regime

In figures 2–4, the internuclear distance is the equilibrium distance, i.e., $R = 2$ au and the electric field amplitude is $F_0 = 1$ au, thus placing the interacting system quite far from the perturbation regime. The fivefold differential ionization probability is examined there as a

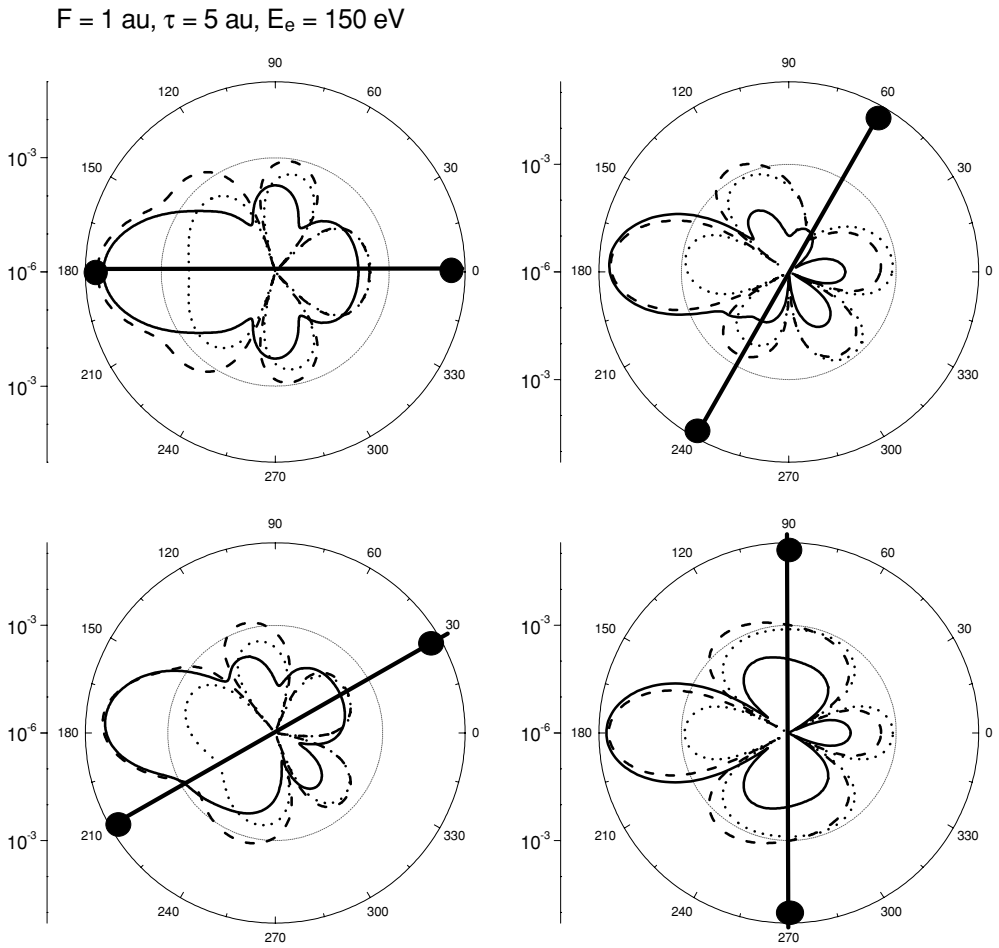

Figure 2. FDIPs for various molecular orientations and an electron ejected at 150 eV. The direction of the external electric field is 0°. The internuclear distance is $R = 2$ au. Full line: CV1 calculation; dashed line: TEC approximation; dotted line: interference factor (see text, equation (34)).

function of the electron ejection angle θ, for various energies of ejected electrons and a few molecular orientations between 0° and 90°.

In figure 2, the electron energy E_e is set to 150 eV and the internuclear axis is rotated from 0° to 90° by steps of 30°. We compare results of present CV1 molecular theory (solid line) defined by equations (22)–(24*a*) and (24*b*) to the TEC approximation (dashed line) defined by equation (32). Let us recall that the latter was already employed to study molecular ionization by impacts of electrons (Stia *et al* 2003) and heavy ions (Laurent *et al* 2002). In both present calculations, FDIPs show a prominent lobe in the backward direction. Such a lobe is characteristic of the dominant influence of a strong field at its maximum intensity. However, the secondary lobes that appear at different angles are connected to the FDIP lobes of the perturbation regime. As the molecular axis rotates, the electron emission pattern follows the rotation with the exception of the main backward lobe, which remains in the same direction. A plot of the (scaled) interference factor

$$\cos^2[(\vec{q} - \vec{k}) \cdot \vec{\rho}/2] \tag{34}$$

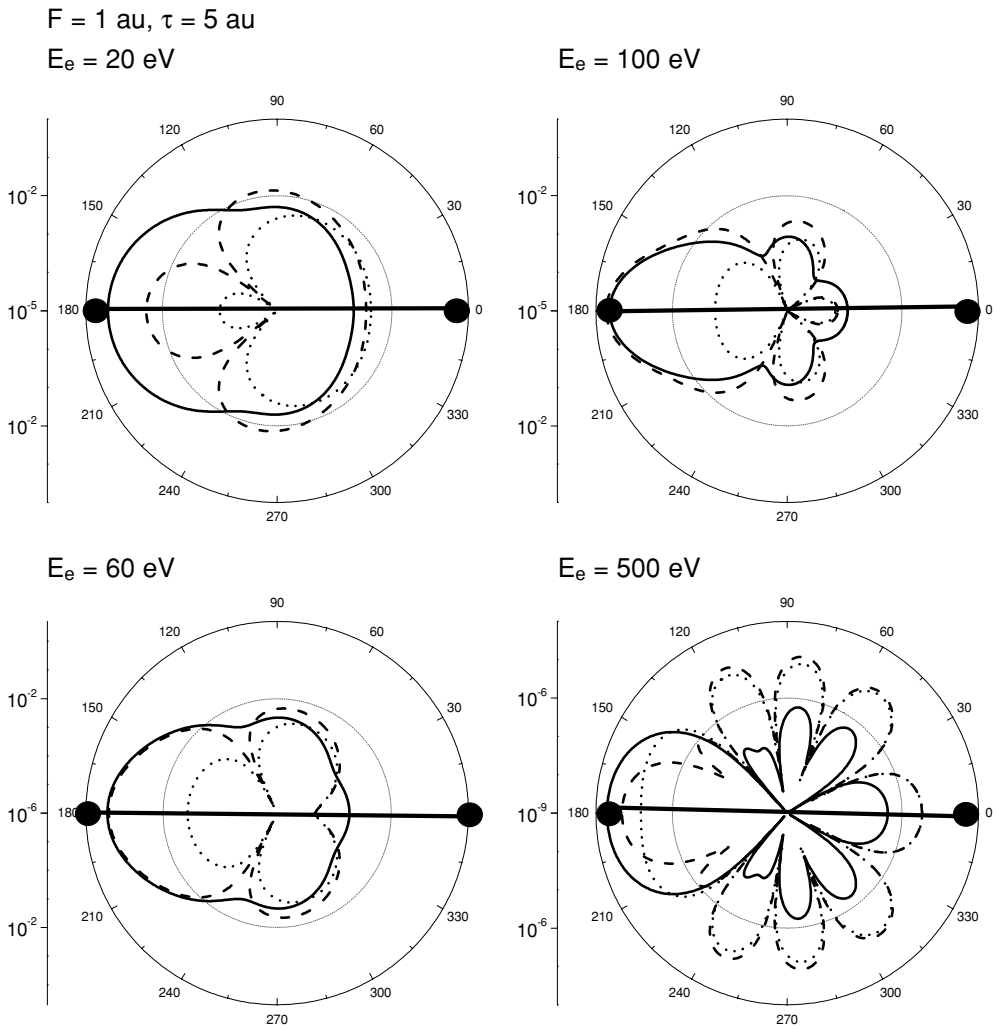

Figure 3. FDIPs for an electron ejected at various energies from a molecule whose axis is parallel to the external electric field directed towards 0°, and whose internuclear distance is $R = 2$ au. Same notation as figure 2.

(dotted line) in the same figure shows that this behaviour of the pattern is the signature of interference between electron emissions from the two nuclei. This conclusion can readily be checked for molecular orientations along 0° and 90°. But it might be less obvious at the intermediate orientations for which the secondary lobes given by CV1 are more oriented in the backward direction than TEC maxima. Moreover, at $\theta_\rho = 60°$ we find that CV1 predicts a maximum along this orientation, at variance with TEC that shows a minimum there. Such discrepancies are evidence for significant higher-order contributions in the expansion of $e^{-i\vec{Q}\cdot\vec{\rho}}$ in crescent powers of $\vec{Q}\cdot\vec{\rho}$ (see text between equations (27) and (28)). Indeed, all the contributions above the 0th-order are neglected in TEC whereas they are all taken into account in CV1.

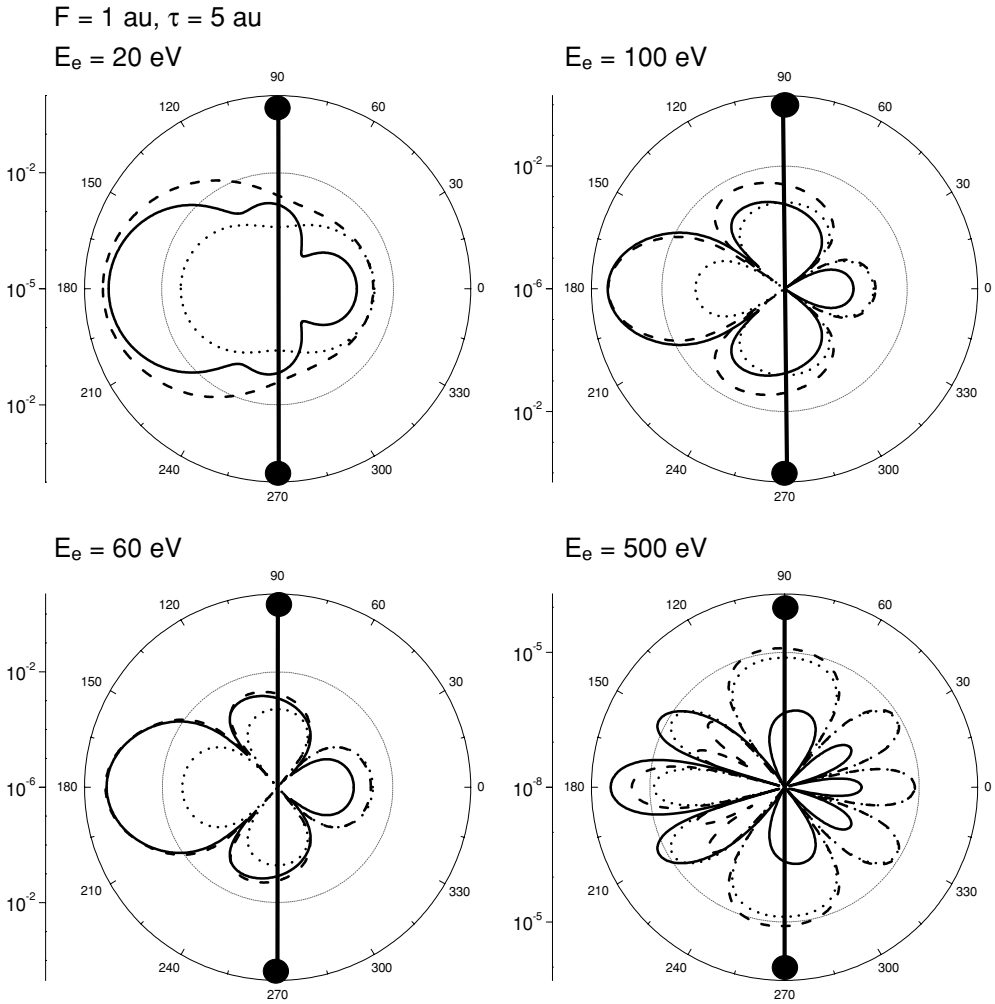

Figure 4. Same as figure 3 but with a molecular axis perpendicular to the electric field.

In figures 3 and 4, one considers two molecular orientations $\theta_\rho = 0^\circ$ and $\theta_\rho = 90^\circ$ respectively. Molecular FDIPs are reported there as functions of the ejected electron angle θ_e for four electron ejection energies, $E_e = 20$, 60, 100 and 500 eV.

To investigate whether nodes show up or not, we first consider the lowest energy $E_e = 20$ eV. At this particular energy with an internuclear axis parallel to the polarization, equation (34) and TEC calculations predict two nodes in FDIP at the same ejection angle whereas CV1, that is a slowly varying function, does not show any node (figure 3). The situation is the opposite for a perpendicular orientation (figure 4): neither TEC, nor equation (34) shows any node whereas CV1 presents two absolute and two relative minima.

In general, for a molecular axis parallel or perpendicular to the polarization, CV1 exhibits smooth minima near the nodes predicted by TEC. There is a single exception at $E_e = 60$ eV with a parallel orientation, where CV1 shows a maximum at $\theta_e = 0^\circ$ whereas TEC predicts a minimum. Figures 3 and 4 indicate that, when the electron energy increases, new FDPI lobes are looming up for these two particular orientations of the molecular axis.

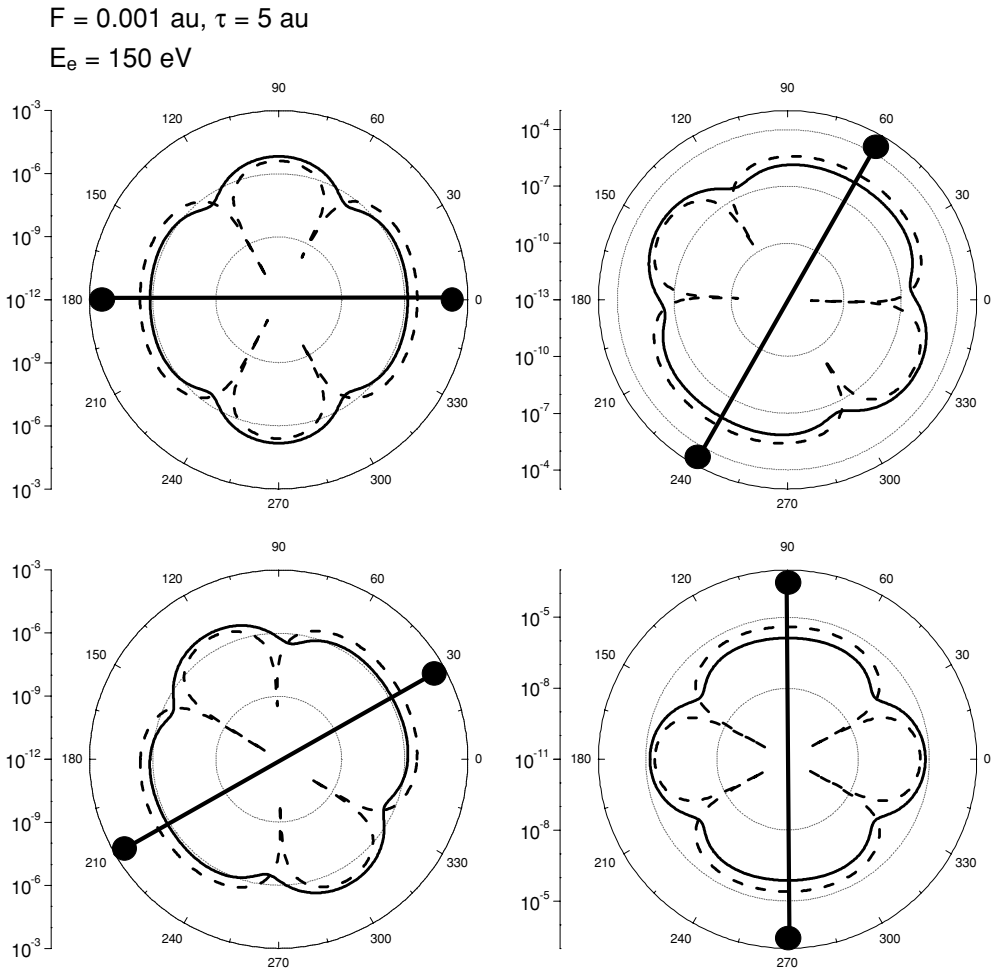

Figure 5. FDIPs for an electron ejected at 150 eV for different molecular orientations and an internuclear distance $R = 2$ au. Full line: CV1 calculation; dashed line: TEC approximation.

With a parallel orientation, we observe 2, 3, 4 and 8 nodes in the FDIP, for E_e = 20, 60, 100 and 500 eV respectively (figure 3). For a perpendicular molecular orientation (figure 4), this increasing series is different: for the above-mentioned electron energy sequence, the electron angular distribution shows 0, 4, 4 and 8 nodes respectively. For the highest energy 500 eV, both TEC and CV1 display almost the same lobe structure, with the exception of the two minima predicted by TEC at $\theta_e = 150^\circ$ and 210°. These minima do not appear, neither in CV1, nor in the interference factor. They are connected to the particular structure of the TEC amplitude. The latter is defined in equation (32) as the product of the interference factor times the atomic ionization probability, which is strongly peaked in the backward direction.

Finally, it is worth noting that the particular orientations of the molecule in figures 3 and 4, lead to diagrams that are all symmetrical with respect to the direction of the pulse polarization. Such a result stems from the axial symmetry of the system with respect to the polarization direction when the molecular axis is, either parallel, or perpendicular to this direction.

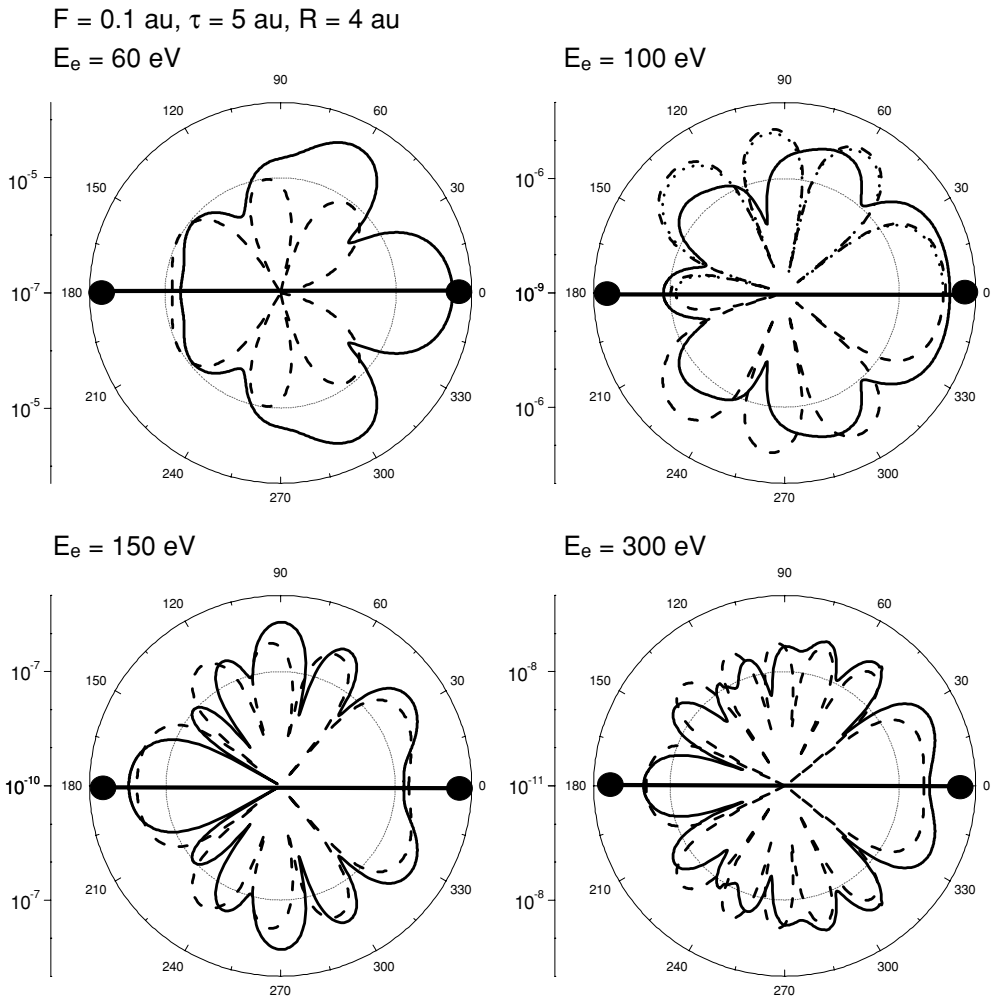

Figure 6. FDIPs for an electron ejected at various energies from a molecule whose internuclear distance is $R = 4$ au and whose axis is parallel to the electric field. Same notation as figure 5.

3.2. Perturbation regime

In order to get close to the photoionization limit, we now look at the behaviour of FDIPs for a much smaller electric field. Beforehand, let us point out that an interference factor similar to (34) also appears in other processes leading to molecular ionization. On the one hand, the appropriate interference factor for photoionization is obtained by setting $\vec{q} = 0$ in (34) (Walter and Briggs 1999). On the other hand, for electron impact ionization $-\vec{q}$ represents the transferred momentum to the ejected electron (Stia *et al* 2002). Even for molecular ionization by fast heavy ions, it is possible to find an expression similar to (32) with a factor in the square-modulus of the transition matrix that is a function of the transverse momentum transfer η (Laurent *et al* 2002). In that latter case however, interferences are somewhat damped by the integration over η.

Predictions with the weak field $F_0 = 10^{-3}$ au are displayed in figure 5. One observes that both CV1 and TEC approximations provide electron emission diagrams always symmetric

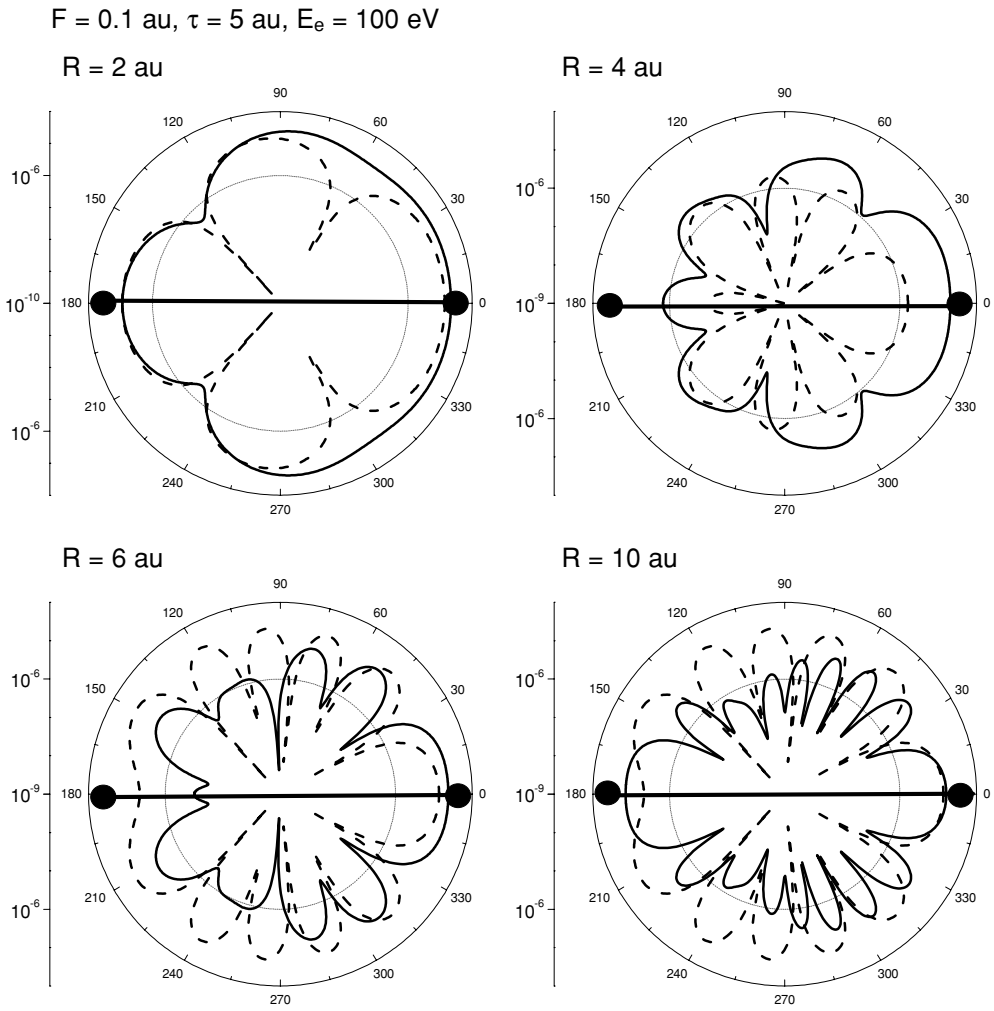

Figure 7. FDIPs for an electron ejected at 100 eV from a molecule whose internuclear distance increases, the molecular axis being parallel to the electric field. Same notation as figure 5.

with respect to the molecular axis. These diagrams looks like being stuck to the molecular reference frame. It just means that the external field is too weak to affect the symmetry of the unperturbed molecular ion. Qualitatively, predictions made by both approaches are similar. As usual, CV1 provides relative minima in place of the nodes predicted by TEC. However, there are large quantitative differences. Indeed, to be reported on the figure, TEC values are divided by 100. Nevertheless, the interference factor arising from the simple picture of the TEC approximation still appears to be a useful guide to explain lobe structures in FDIPs.

3.3. Dependence on the internuclear distance

The FDIP lobe structure depends on both the internuclear orientation and the internuclear distance. We investigate now the evolution of the electronic distribution as a function of the the internuclear separation R. In figures 6 and 7, FDIP predictions are reported for a not too strong external electric field $F_0 = 0.1$ au parallel to the molecular axis.

Calculations of FDPI reported in figure 6 are carried out for $R = 4$ au. Although a qualitative agreement is found between CV1 and TEC theories for electron ejected along the molecular axis, discrepancies appear for other emission angles. Further, there is no quantitative agreement since TEC results have to be divided by 100 to be reported in emission diagrams of figures 6 and 7. Now, it is interesting to compare diagrams drawn in figures 2 and 3 for $R = 2$ with diagrams of figure 6 where $R = 4$. For the same molecular orientation and the same electron ejection energy, more lobes show up in figure 6. Although field intensities are different, such a feature suggests that the lobe structure of FDIP could provide us with information on the dynamics of nuclei in a molecule. Subsequent calculations reported in figure 7 support this suggestion.

In figure 7, four FDIP diagrams are displayed for electrons ejected at 100 eV in each case. As in figure 6, the electric field amplitude is $F_0 = 0.1$ au and the molecular axis is parallel to the external electric field. FDIP calculations are performed for growing internuclear distances $R = 2$, 4, 6 and 10 au. Agreement between CV1 and TEC approaches is similar to figure 6, again with TEC results multiplied by 10^{-2}. According to the figure, the larger the internuclear distance, the more numerous the lobes. This is consistent with equation (34), which predicts a number of FDIP lobes that grows linearly with $k\rho$ while it is independent of the field strength. Thus, for a fixed molecular orientation, it is possible to have a good indication of the internuclear distance by counting the number of lobes in the FDIP of electrons with the same energy. Therefore, the observation of the lobe structure of FDIP might be a way to trace the dynamics of molecular vibrational states.

Finally, it is noteworthy that FDIP patterns shown in figures 6 and 7 look more similar to the corresponding patterns exhibited in figures 2–4 than to those reported in figure 5. It is no wonder since $F_0 = 0.1$ au sets the interacting system quite outside the perturbation regime.

4. Concluding remarks

Fivefold differential angular distributions of ejected electrons have been studied as functions of both molecular orientation and internuclear distance using an extension of the CV1 theory to molecular ionization by ultra-short electromagnetic pulses. Both non-perturbative and perturbative situations have been examined. In the non-perturbative case, the interference pattern shows up but a prominent lobe dominates the angular distribution in a direction opposite to the electric field polarization. In contrast, in the perturbative case, the interference structure can be related to that obtained in molecular ionization by fast electron impacts. The interference pattern can be obtained easily by means of the so-called two-effective centres (TEC) approximation that may be derived from the full CV1 theory. TEC does provide a simple and useful guide to understand the otherwise complex lobe structure of the FDIP. However, there are some numerical discrepancies, particularly in non-perturbative situations. It is no wonder since we showed that the main contributions to the full CV1 amplitude, come from the neighbourhoods of $\vec{Q} = \vec{0}$ and $\vec{Q} = \vec{k} - \vec{q}$ (see equation (23). For large values of the electric field F_0, the two peaks, that are far apart, contribute to the full CV1 amplitude whereas the TEC transition amplitude is only determined a contribution at $\vec{Q} = \vec{0}$.

The situation is very different in perturbation conditions because q is small. Therefore, depending on $\vec{k}$, the value of $\|\vec{k} - \vec{q}\|$ is generally much smaller than in the non-perturbative case, thus preventing from getting two well-separate peaks in (23).

Theoretically, a connection has been established between the angular distributions of ejected electrons and Young-type interferences. These distributions have been shown to strongly depend on the internuclear distance. Further, for a fixed molecular orientation and a

given ejected electron energy, the number of FDIP lobes appears to be roughly proportional to the internuclear distance.

Acknowledgments

The collaboration between the group 'XUV harmonics, ultra-short processes and applications' at CELIA (Bordeaux, France) and DF, FCEyN (Universidad de Buenos Aires, Argentina) was partially supported by the programme ECOS/CONICYT, Grant No. C03E01. Support by the Universidad de Buenos Aires under grant X259 is also acknowledged.

References

Cohen H D and Fano U 1966 *Phys. Rev* **150** 30
Cormier E and Lambropoulos P 1997 *J. Phys. B: At. Mol. Opt. Phys.* **30** 77
Dollard J D 1964 *J. Math. Phys.* **5** 729
Duchateau G, Cormier E, Bachau H and Gayet R 2001 *Phys. Rev.* A **63** 053411
Duchateau G, Cormier E and Gayet R 2000a *Eur. Phys. J.* D **11** 191
Duchateau G, Cormier E and Gayet R 2002 *Phys. Rev.* A **66** 023412
Duchateau G, Cormier E and Gayet R 2003 *J. Mod. Opt.* **50** 331
Duchateau G and Gayet R 2001 *Phys. Rev.* A **65** 013405
Duchateau G, Illescas C, Pons B, Cormier E and Gayet R 2000b *J. Phys. B: At. Mol. Opt. Phys.* **33** L571
Ellert Ch and Corkum P B 1999 *Phys. Rev.* A **59** R3170
Faisal F H M 1973 *J. Phys. B: At. Mol. Phys.* **6** L89
Galassi M E, Rivarola R D, Fainstein P D and Stolterfoht N 2002 *Phys. Rev.* A **66** 052705
Jain M and Tzoar N 1978 *Phys. Rev.* A **18** 538
Joulakian B, Hanssen J, Rivarola R and Motassim A 1996 *Phys. Rev.* A **54** 1473
Keldysh L V 1965 *Sov. Phys. JETP* **20** 1307
Kondorskiy A D and Presnyakov L P 2001 *J. Phys. B: At. Mol. Opt. Phys.* **34** L263
Laurent G, Fainstein P D, Galassi M E, Rivarola R D, Adoui L and Cassimi A 2002 *J. Phys. B: At Mol. Opt. Phys.* **35** L495
Lein M, Marangos J P and Knight P L 2002a *Phys. Rev.* A **66** 051404(R)
Lein M, Hay N, Velotta R, Marangos J P and Knight P L 2002b *Phys. Rev. Lett.* **88** 183903
Litvinyuk I V, Lee K F, Dooley P W, Rayner D M, Villeneuve D M and Corkum P B 2003 *Phys. Rev. Lett.* **90** 233003
Macri P A, Miraglia J E and Gravielle M S 2003 *J. Opt. Soc. Am.* B **20** 1801
Misra D, Kadhane U, Singh Y P, Tribedi L C, Fainstein P D and Richard P 2004 *Phys. Rev. Lett.* **92** 153201
Moshammer R *et al* 1997 *Phys. Rev. Lett.* **79** 3621
Muller H G and Kooiman F C 1998 *Phys. Rev. Lett.* **81** 1207
Muth-Böhm J, Becker A and Faisal F H M 2000 *Phys. Rev. Lett.* **85** 2280
Muth-Böhm J, Becker A, Chin S L and Faisal F H M 2001 *Chem. Phys. Lett.* **337** 313
Nisoli M, de Silvesti S, Svelto O, Szipöcs R, Ferencz K, Spielmann Ch, Sartania S and Krausz F 1997 *Opt. Lett.* **22** 522
Nordsieck A 1954 *Phys. Rev.* **93** 785
Reid K L 2003 *Ann. Rev. Phys. Chem.* **54** 397
Reiss H R 1980 *Phys. Rev.* A **22** 1786
Rodriguez V D, Cormier E and Gayet R 2004 *Phys. Rev.* A **69** 053402
Rodriguez V D and Falcon C A 1990 *J. Phys. B: At. Mol. Opt. Phys.* **23** L547
Seideman T 2002 *Annu. Rev. Phys. Chem.* **53** 41
Serov V V, Joulakian B B, Pavlov D V, Puzynin I V and Vinitsky S I 2002 *Phys. Rev.* A **65** 062708
Spanner M, Smirnova O, Corkum P B and Ivanov M Y 2004 *J. Phys. B: At. Mol. Opt. Phys.* **37** L243
Stia C R, Fojon O A, Weck P F, Hanssen J, Joulakian B and Rivarola R D 2002 *Phys. Rev.* **66** 052709
Stia C R, Fainstein P D, Galassi M E, Rivarola R D, Adoui L and Cassimi A 2003 *J. Phys. B: At. Mol. Opt. Phys.* **36** L257
Stolterfoht N *et al* 2001 *Phys. Rev. Lett.* **87** 023201
Walter M and Briggs J S 1999 *J. Phys. B: At. Mol. Opt. Phys.* **32** 2487
Weber Th *et al* 2004 *Phys. Rev. Lett.* **92** 163001
Wells E, De Witt M J and Jones R R 2002 *Phys. Rev.* A **66** 013409
Weck P, Fojon O A, Hanssen J, Joulakian B and Rivarola R D 2001 *Phys. Rev.* A **63** 042709